Check for updates

Research article

I·M3 Institute of Materials, Minerals & Mining

Ironmaking & Steelmaking
1–14
© The Author(s) 2026
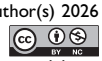
Article reuse guidelines:
sagepub.com/journals-permissions
DOI: 10.1177/03019233261502167
journals.sagepub.com/home/ist
Sage

# Development and validation of a one-dimensional mathematical model for cold rolling simulation with mixed lubrication

**Valentina Colla[1], Orlando Toscanelli[1], Alice Petrucciani[1], Leon Jacobs[2] and Tommaso Grossi[1]**

## Abstract

Cold rolling of steel strip is a complex metal forming process involving intrinsically coupled mechanical, tribological, and thermal phenomena that challenge the development of accurate and computationally efficient predictive models. A comprehensive one-dimensional mathematical model for cold rolling simulation is developed and validated against experimental data from pilot mill trials. The model integrates elasto-plastic strip mechanics, mixed lubrication, elastic roll deformation, and thermal effects in a fully coupled Python framework, achieving computational times of a few seconds. A preliminary two-dimensional finite element study validates the one-dimensional mechanical assumption. The validation against Tata Steel pilot mill data shows excellent agreement, with maximum relative errors below 10% and average relative errors of approximately 5% for rolling force predictions.

## Keywords

cold rolling, mathematical modeling, mixed lubrication, hydrodynamic lubrication, Reynolds equation, asperity flattening, roll deformation

Received: 18 January 2026; accepted: 11 October 2026

## Introduction

Cold rolling of steel strip represents one of the most complex metal forming processes from both tribological and mechanical perspectives, as it involves strong coupling of multiple physical phenomena occurring at vastly different scales.[1,2] The mechanical behavior encompasses the elasto-plastic deformation of the strip material, characterized by strain hardening,[3] and the elastic response of the work rolls under contact loads.[4,5] Simultaneously, the contact interface between roll and strip exhibits mixed lubrication conditions, where hydrodynamic lubricant films coexist with areas of asperity contact.[6,7] This tribological complexity is further compounded by thermal effects arising from plastic deformation and frictional dissipation, which significantly alter material properties and lubricant viscosity.[8]

The development of accurate yet computationally efficient models for cold rolling has been pursued intensively over several decades, driven by industrial demands for tighter tolerances on strip thickness, improved surface quality, and optimized process parameters.[1,9] The advent of finite element methods enabled more detailed three-dimensional analyses,[10–12] yet the computational cost remains prohibitive for real-time applications or extensive parametric studies.[13] One-dimensional models offer an attractive compromise, capturing the essential physics along the rolling direction while maintaining computational efficiency.[4,14] However, the validity of such models rests critically on the assumption that stress and strain fields are approximately homogeneous through the strip thickness, an approximation that requires careful validation particularly for the severe reductions often encountered in cold rolling.[15,16]

The lubrication regime in cold rolling typically falls within the mixed or thin-film domain, where the lubricant film thickness is comparable to the combined surface roughness of roll and strip.[6,17] Under these conditions, load is transmitted partly through hydrodynamic pressure in lubricant pockets and partly through direct asperity contact.[18,19] Accurate modeling of this mixed lubrication regime necessitates solving the Reynolds equation for the lubricant flow while accounting for asperity deformation,[7,20] Piezo-thermal effects on viscosity,[8,21] and the influence of surface topography.[22,23]

This paper presents the development and validation of the Cold Rolling 1D Simulator (CR1S), a comprehensive model that integrates these coupled phenomena in a

[1]TeCIP Institute, Scuola Superiore Sant'Anna, Pisa, Italy
[2]Tata Steel, Research & Development, Velsen-Noord, The Netherlands

**Corresponding author:**
Tommaso Grossi, TeCIP Institute, Scuola Superiore Sant'Anna, Via Moruzzi 1, 56124 Pisa, Italy.
Email: tommaso.grossi@santannapisa.it

| Symbol | Description | Unit | Symbol | Description | Unit |
|---|---|---|---|---|---|
| $\bar{\sigma}$ | Equivalent flow stress | MPa | $h_t$ | Local lubricant film thickness | $\mu$m |
| $\varepsilon_p$ | Equivalent plastic strain | – | $Q$ | Volumetric flow rate per unit width | $m^2\,s^{-1}$ |
| $\dot{\varepsilon}_p$ | Equivalent plastic strain rate | $s^{-1}$ | $R_q$ | Combined RMS surface roughness | $\mu$m |
| $a$, $b$, $n$, $c$, $m$ | Johnson–Cook hardening parameters | various | $\phi_x$, $\phi_s$ | Pressure and shear flow factors | – |
| $\dot{\varepsilon}_0$ | Reference strain rate | $s^{-1}$ | $v_r$, $v_s$ | Roll and strip surface velocities | $m\,s^{-1}$ |
| $T_r$, $T_{melt}$ | Reference and melting temperatures | °C | $\tau_l$, $\tau_a$ | Lubricant viscous and asperity friction shear stresses | MPa |
| $\sigma_x$, $\sigma_y$ | Normal stresses (rolling and thickness directions) | MPa | $R$, $R'$ | Undeformed and flattened work roll radius | mm |
| $\tau$ | Interface shear stress | MPa | $\nu$, $E$ | Poisson's ratio and Young's modulus of roll material | – / GPa |
| $t$, $t_{in}$, $t_{out}$ | Local, inlet, and outlet strip thickness | mm | $P'$ | Rolling force per unit width | $N\,mm^{-1}$ |
| $t_m$ | Mean strip thickness | mm | $\delta_{in}$, $\delta_{out}$ | Elastic inlet/outlet zone corrections | mm |
| $\sigma_{in}$, $\sigma_{out}$ | Inlet and outlet strip tensions | MPa | $T_s$, $T_l$ | Strip and lubricant temperatures | °C |
| $p$ | Roll pressure | MPa | $\beta_s$ | Taylor–Quinney coefficient | – |
| $A$ | Real contact area fraction | – | $\beta_l$ | Lubricant heat partition coefficient | – |
| $p_l$ | Hydrodynamic lubricant pressure | MPa | $\dot{W}_p$ | Plastic work rate per unit volume | $W\,m^{-3}$ |
| $p_a$ | Average asperity contact pressure | MPa | $\rho_s$, $c_s$ | Strip density and specific heat | $kg\,m^{-3}$ / $J\,kg^{-1}K^{-1}$ |
| $\eta$ | Dynamic viscosity | Pa s | $\rho_l$, $c_l$ | Lubricant density and specific heat | $kg\,m^{-3}$ / $J\,kg^{-1}K^{-1}$ |
| $\eta_0$ | Reference viscosity | Pa s | $\beta$ | Thermo-viscous coefficient | $K^{-1}$ |
| $\alpha$ | Piezo-viscous coefficient | $Pa^{-1}$ | $M$ | Rolling torque | N m |

computationally efficient framework. The model was developed within the RollOilFree II project (RFCS grant agreement 101112433[24]), whose objective is the industrial application of oil-free lubricants (OFLs) in steel cold rolling, for which the ability to predictively simulate the effect of lubricant physical properties on cold rolling performance is a key requirement.

A key feature of the present work is the development of a fully customizable computational framework that provides complete control over all aspects of the numerical procedure and constitutive modeling. The CR1S presented here is built from scratch upon open-source Python libraries, with performance-critical sections accelerated through `numba` just-in-time compilation, achieving computational times of a few seconds per simulation while maintaining full transparency and control of the solution algorithms. More importantly, the model architecture is designed to allow straightforward substitution and modification of constitutive relationships for both the strip material and the lubricant, enabling systematic exploration of novel lubricant formulations with non-standard viscosity–pressure–temperature dependencies. This customizability is particularly valuable for emerging applications such as OFLs, where conventional empirical correlations developed for oil emulsions may not apply, and the ability to rapidly implement and test alternative rheological models becomes essential for lubricant optimization and process design. Furthermore, the modular structure facilitates integration of advanced constitutive models for materials exhibiting complex hardening behavior, anisotropy, or rate-dependent effects, without requiring modifications to the core solution algorithms.

The main contributions of the present work are: (i) the development of CR1S, a fully customizable one-dimensional cold rolling simulator built on open-source Python libraries with `numba` just-in-time compilation; (ii) the validation of the one-dimensional mechanical assumption through dedicated two-dimensional finite element analyses covering all experimental conditions; and (iii) quantitative validation against pilot mill trial data for three different steel grades.

This paper is organized as follows. First, the current state of the art in cold rolling modeling is reviewed, categorizing approaches by spatial dimensionality and identifying their respective advantages and limitations. Then, preliminary two-dimensional finite element analyses are described that validate the through-thickness homogeneity assumptions underlying the one-dimensional formulation. Subsequently, a detailed description of the CR1S model is provided, including the treatment of strip mechanics, mixed lubrication, lubricant hydrodynamics, roll elasticity, and thermal coupling. Finally, the validation of CR1S predictions against pilot mill trial data is presented, demonstrating its predictive capabilities and discussing sensitivity to key process parameters.

## State of the art in cold rolling modeling

The numerical simulation of cold rolling processes has evolved considerably over the past five decades, driven by the need to predict and control increasingly stringent product specifications.[1,2,25] Models can be broadly categorized by their spatial dimensionality and the level of physical detail incorporated, with trade-offs between accuracy, generality, and computational cost.

Throughout this classification, and consistently with established usage in the rolling literature,[1,4,14,26] *dimensionality* denotes the number of independent spatial coordinates over which the governing differential equations for the strip's mechanical, thermal, and tribological state are resolved, not the number of physical directions along which derived or resultant quantities such as force, torque, or tension are defined. One-dimensional (slab) models integrate a system

of ordinary differential equations along the single rolling-direction coordinate $x$ under the plane-sections assumption of through-thickness homogeneity; two-dimensional models additionally resolve the through-thickness coordinate $y$ as an independent variable, typically via plane-strain finite element discretization; three-dimensional models further resolve the transverse (width) coordinate $z$. The same convention underlies, for instance, the classification of Euler–Bernoulli beam theory as one-dimensional, notwithstanding that it predicts loads and stresses acting in more than one physical direction. Rolling force per unit width, torque, and forward slip are, in this sense, outputs obtained by integrating or post-processing the $x$-dependent state variables of a one-dimensional formulation, and not evidence that additional spatial coordinates are resolved within its governing equations.

### Three-dimensional models

Full three-dimensional finite element models represent the most comprehensive approach, capable of capturing the complete stress and strain fields in both strip and rolls, including variations in the transverse direction.[10–12] Such models are essential for analyzing phenomena such as width spread, edge shape evolution, and transverse variations in strip thickness (crown and profile).[11] However, the computational cost is substantial, particularly when incorporating realistic material models with anisotropic hardening,[3] detailed surface topography for tribological analysis, and thermal coupling.[13,27] It is well established that the steady-state three-dimensional solution of the cold rolling problem is well approximated by two-dimensional simulations under the plane strain assumption, except at the strip edges, whose spatial extent is very limited compared to the overall width.[12]

Recent advances in steady-state finite element formulations and novel substructuring approaches have significantly reduced computational requirements.[10,16] Nevertheless, for parametric studies or online process control, even optimized three-dimensional models remain impractical due to solution times typically measured in hours or days.

### Two-dimensional models

Plane strain two-dimensional models, which neglect width variations and assume conditions prevailing across the strip width (i.e., excluding edge effects), have proven highly successful for analyzing cold rolling of wide strips.[11–13] These models capture the essential mechanical coupling between strip deformation and roll flattening while maintaining manageable computational costs.[27] With regard to the mechanical simulation of the deformation process, including through-thickness variations in the solution fields and the prediction of effects such as work roll deflection and residual stresses,[15,16] two-dimensional models represent the current state of the art.

The use of the arbitrary Lagrangian–Eulerian (ALE) formulation has proven particularly effective for addressing the steady-state rolling problem.[13,27] This approach allows efficient simulation of the continuous process while avoiding the computational expense of transient startup simulations. However, the use of finite element software poses significant challenges for coupling with the fluid dynamics of the lubricant and its interaction with surface geometrical details at the microscale.[20,28] There are examples in the literature where the contact between the strip and work roll surfaces has been modeled by coupling two-dimensional finite element simulations with the solution of the Reynolds equation for thin viscous fluid films, with the two solutions iteratively updated until convergence is achieved.[13]

### One-dimensional models

One-dimensional models, which assume that stresses vary only in the rolling direction and are uniform through the strip thickness, offer the most attractive computational efficiency while retaining the ability to predict global quantities such as rolling force, torque, and forward slip with reasonable accuracy.[1,4,14] The key assumption underlying these models is that the ratio of strip thickness to contact length is sufficiently small that plane sections remain approximately plane and perpendicular to the strip surface. These models are widely adopted in the rolling industry because they offer a strong balance between predictive accuracy, computational efficiency, and simplicity in methodology.[1,9]

The first model of this kind dates back to von Karman's 1925 work,[14] in which he formulated what is now known as the von Karman equation. This equation was subsequently solved using various methods and under different constitutive assumptions for the interface stresses. Building on this pioneering work, and with the advent of numerical simulation tools, successive refinements have been introduced to the underlying physics in order to achieve increasingly accurate representations of experimental observations.

Hitchcock,[5] followed by Bland and Ford,[4] introduced the capability to account for the deformation of the work rolls. Contributions have been made by incorporating hydrodynamic lubrication into the modeling.[20] Significant advances were achieved in explicitly simulating the lubricant's fluid dynamics by solving the Reynolds equation at the interface.[7,8] The problem of asperity flattening was investigated by formulating models that describe the increase in the real contact area at the interface due to the flattening of surface roughness asperities.[6,18,19,29] These efforts culminated in their comprehensive incorporation into more recent one-dimensional models, such as those developed by Jacobs,[30–32] Marsault,[33] Stephany,[34,35] Carretta,[36,37] and Boemer.[26] These models account for all the afore-mentioned phenomena, along with thermal modeling,[21,38] and even offer the possibility of iteratively coupling the one-dimensional framework with an asperity flattening model derived from a two-dimensional finite element simulation, rather than relying on an analytical formulation.[26] In terms of accuracy with respect to experimental results, the most promising outcomes have been achieved precisely with these one-dimensional models, at least for predicting key variables such as rolling force and rolling torque.[26,30,36] Naturally, this excludes phenomena where through-thickness variations in the solution fields become significant.

### Data-driven and hybrid modeling approaches

Beyond the three physics-based categories discussed above, an increasingly active line of research pursues fast rolling

force and forward slip prediction through machine learning. A first family trains surrogate models—polynomial response surfaces or artificial neural networks—on databases of high-fidelity finite element simulations, trading offline database generation cost for near-instantaneous online evaluation.[39] A second family is purely data-driven, fitting regression or neural-network models directly to industrial process data collected from operating mills.[40] A third, hybrid family combines a mechanistic model with a machine-learning correction term trained to compensate for the residual discrepancy with respect to measured or simulated data, an approach that has also been applied specifically to rolling schedule presetting.[41–43]

These approaches share the property that their accuracy is, by construction, contingent on the range of process conditions, materials, and—for industrial-data-driven models—mills represented in the training set; extrapolation beyond this envelope is not guaranteed and is typically not verifiable without additional experimental data. The one-dimensional formulation presented here follows a complementary route: instead of being trained to reproduce a specific dataset, its constitutive inputs—the Johnson–Cook hardening parameters, the lubricant rheological coefficients, and the surface roughness—are measured independently of the rolling force and torque data used for validation (as detailed in the lubrication section). Its predictive capability for new lubricant formulations therefore rests on the transferability of the underlying physical laws, which is precisely why this approach was adopted for the present application: at the time of writing, no operational dataset of industrial cold rolling with OFLs exists from which a data-driven or surrogate model could be trained. A systematic comparison of the present physics-based approach against data-driven or hybrid alternatives, once sufficient OFL process data becomes available, is identified here as a direction for future work.

## Validation of one-dimensional assumptions through finite element analysis

### Finite element model formulation

The validity of one-dimensional mechanical models for cold rolling rests fundamentally on the assumption that stress and strain fields are approximately uniform through the thickness of the strip. While this assumption is intuitively reasonable for rolling of thin strip with large diameter rolls, it requires quantitative verification, particularly for the finite reductions typical of industrial practice where gradients through the thickness may become significant.[15,16] The two-dimensional finite element analyses presented in this section were therefore conducted to verify this assumption for the specific experimental conditions that would subsequently be used for model validation (detailed in the experimental validation section).

To assess the homogeneity of through-thickness fields, a series of two-dimensional plane strain finite element analyses were conducted using ANSYS Mechanical APDL (shown in Figure 1). The model is built using the ANSYS Mechanical finite element solver and does not explicitly simulate fluid dynamics. The contact between surfaces is modeled in a simplified manner using contact elements with friction, without explicitly representing the lubricant film thickness.

The strip material was modeled including its elastic behavior and using a plastic constitutive law with isotropic hardening according to a classic Johnson–Cook model (equation (1)):

$$\bar{\sigma} = \left(a + b\varepsilon_p^n\right)\left(1 + c\ln\frac{\dot{\varepsilon}_\mathrm{p}}{\dot{\varepsilon}_0}\right)\left(1 - \left(\frac{T - T_\mathrm{r}}{T_\mathrm{melt} - T_\mathrm{r}}\right)^m\right)$$

where $\bar{\sigma}$ is the yield stress, $a$ and $b$ are material constants, $n$ is the strain hardening exponent, $c$ is the strain rate sensitivity coefficient, $m$ is the thermal softening exponent, $\dot{\varepsilon}_0$ is a reference strain rate, $T_\mathrm{r}$ is a reference temperature, and $T_\mathrm{melt}$ is the melting temperature of the material.

Material parameters were selected to represent typical low-carbon steel grades used in cold rolling applications. The work rolls were treated as elastic bodies with prescribed rotation, and contact between roll and strip was enforced using the penalty method with a Coulomb friction coefficient.

To validate the through-thickness homogeneity assumption for conditions representative of the experimental pilot trials described in the experimental section (see Tables 1–3), a parametric study was conducted. The finite element simulations were performed for all experimental cases listed in Tables 1 to 3, encompassing reduction ratios from 21% to 38%, strip thicknesses from 0.23 to 2.52 mm, and roll radius to initial strip thickness ratios from approximately 79 to 862. Since the tribological properties of the lubricant (particularly the effective coefficient of friction at the interface) were not precisely known a priori, each experimental configuration was analyzed with friction coefficients varying from 0.05 to 0.15 to account for this uncertainty. For each combination of parameters, the distributions of normal stress, equivalent plastic strain, and hydrostatic pressure were examined along vertical sections at several locations through the roll bite.

### Results and assessment of through-thickness homogeneity

The finite element results reveal that, for all experimental cases examined (corresponding to the conditions listed in Tables 1–3 and the range of friction coefficients tested), the through-thickness variation of stress and strain is remarkably small (as shown in Figures 2 and 3). Figures refer to the worst case in terms of non-uniformity. The normal stress varies by less than 3% across the thickness at all locations, with slightly larger gradients (approximately 5%) occurring near the surfaces due to frictional shear. The equivalent plastic strain distribution shows similar uniformity, with through-thickness variations below 4% except in the immediate vicinity of the neutral point where the stress state transitions (see Figure 4).

These results provide strong support for the one-dimensional approximation in the central region of the roll bite (as demonstrated in Figures 5 and 6), confirming that the assumption of homogeneous through-thickness fields introduces errors substantially smaller than uncertainties in material properties and boundary conditions.[15] It should be noted, however, that the analysis also reveals more

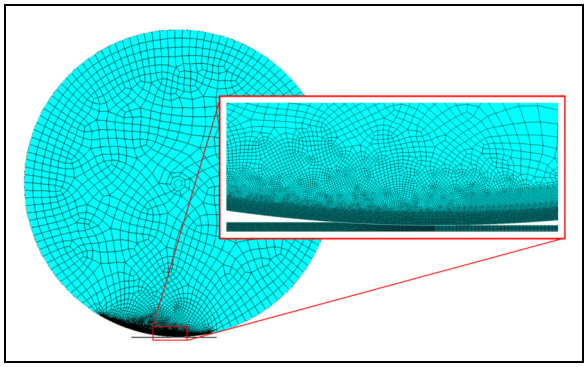

**Figure 1.** Finite element 2D model, with detail of the refined mesh in the contact zone.

significant three-dimensional effects in the inlet region, where elastic contact precedes plastic yielding, and in the outlet region, where elastic springback occurs (see Figure 7). These zones may influence the entry and exit film thicknesses predicted by lubrication models, a consideration that requires attention in the one-dimensional formulation.[7,17]

The validity of the 1D assumption is expected to hold when the contact length is at least three to five times the strip thickness—approximately corresponding to strip thicknesses below 3 mm for a 400-mm-diameter roll and maximum reductions of approximately 40%. This threshold is directly supported by recent asymptotic and finite element benchmark studies of through-thickness stress fields in cold rolling,[16] in addition to being consistent with classical deformation-zone geometry criteria ($\Delta = t_m/L \leq 0.2--0.33$, where $t_m$ is the mean strip thickness and $L$ the contact length) for homogeneous deformation in metal forming.[1,4] It is corroborated directly by the FE parametric study reported in this section, which spans the full range of thicknesses and reductions of the experimental validation dataset (Tables 1–3). For larger reductions, smaller rolls, or non-uniform friction between the two strip surfaces, the through-thickness gradients may become significant and the 1D approximation may require correction or replacement by a 2D model. The FE results presented here, encompassing all experimental conditions of the validation dataset, confirm the adequacy of the assumption within these bounds.

## The CR1S one-dimensional model

### Mechanical behavior of the strip

CR1S integrates models for strip mechanics, mixed lubrication, lubricant hydrodynamics, roll elasticity, and thermal effects within a unified computational framework. The model is formulated as an Initial Value Problem, where the values of the variables before entering the roll bite are evolved through a system of differential equations to obtain the final values at the exit of the deformation zone.

The mechanical behavior of the strip is modeled using the classical Johnson–Cook model,[44] which describes the evolution of the plastic flow stress according to the strain hardening law. This equation enables the modeling of material hardening under varying strain rates and temperatures, making it a convenient choice when these phenomena play a significant predictive role, while still maintaining relative simplicity in its implementation. The Johnson–Cook model has been widely validated for steels under various deformation conditions.[3,44]

**Table 1.** Summary of cold rolling experiments at Tata Steel pilot mill for the soft steel.

| Pass | $t_{in}$ (mm) | $t_{out}$ (mm) | $\sigma_{in}$ (MPa) | $\sigma_{out}$ (MPa) | $v_r$ (m/s) | Force (N/mm) | Torque (Nm) |
|---|---|---|---|---|---|---|---|
| 1 | 2.52 | 1.82 | 31.7 | 55.1 | 4.0 | 7100 | 3000 |
| 2 | 1.82 | 1.30 | 44.1 | 77.0 | 7.0 | 7600 | 2700 |
| 3 | 1.30 | 0.91 | 61.6 | 110.4 | 10.0 | 7700 | 2300 |
| 4 | 0.91 | 0.65 | 88.3 | 153.2 | 11.0 | 7000 | 1600 |

The mechanical model employs the slab method,[4,14] considering equilibrium of a longitudinal strip element in the rolling direction. At each position along the roll bite, the strip thickness is determined by the roll gap geometry, accounting for elastic flattening of the rolls. The plane strain yield condition[45] relates the normal stress in the rolling direction $\sigma_x$ to the vertical normal stress $\sigma_y$ and the material flow stress $\bar{\sigma}$ (equation (2)):

$$\sigma_x - \sigma_y = -\frac{2}{\sqrt{3}}\bar{\sigma}$$

where compressive stresses are taken as negative.

Longitudinal equilibrium of a strip slab of thickness $dx$ gives (equation (3)):

$$\frac{d}{dx}(\sigma_x t) + \sigma_y \frac{dt}{dx} + 2\tau = 0$$

where $\tau$ is the interface shear stress and $t$ is the local strip thickness at a given longitudinal position $x$. Combining these relations with the boundary conditions imposed by back and front tensions yields a differential equation for the roll pressure $p$, which is solved numerically subject to the inlet and outlet conditions.

The flow stress $\bar{\sigma}$ evolves along the roll bite according to the assumed strain hardening law.[3] The equivalent plastic strain is determined from the von Mises criterion under plane strain conditions (equation (4)):

$$\varepsilon_p = \frac{2}{\sqrt{3}} \ln\left(\frac{t_{in}}{t}\right)$$

where $t_{in}$ is the inlet strip thickness. This expression follows from the assumption that elastic strains are negligible compared to plastic strains ($\bar{\varepsilon} = \bar{\varepsilon}_p$), the definition of effective plastic strain rate, and the incompressibility of plastic deformation under plane strain conditions ($\varepsilon_x + \varepsilon_z = 0$ and $\varepsilon_y = 0$), where the thickness strain is $\varepsilon_z = \ln(t(x)/t_{in})$.

### Treatment of mixed lubrication

One of the most complex simulation aspects of the problem is represented by the distribution of contact stresses between the lubricant and the metallic surfaces under mixed lubrication conditions.[6,18] It is assumed that direct contact between the surfaces occurs over a fraction $A$ of the interface area[18,46]; the total interface pressure is partitioned into the fraction $A$ of real contact area where asperities are flattened, and a complementary fraction where the surfaces are separated by a lubricant

**Table 2.** Summary of cold rolling experiments at Tata Steel pilot mill for the hard steel.

| Pass | $t_{in}$ (mm) | $t_{out}$ (mm) | $\sigma_{in}$ (MPa) | $\sigma_{out}$ (MPa) | $v_r$ (m/s) | Force (N/mm) | Torque (Nm) |
|---|---|---|---|---|---|---|---|
| 1 | 1.82 | 1.42 | 55.1 | 70.7 | 4.0 | 7100 | 2200 |
| 2 | 1.42 | 1.12 | 70.7 | 89.5 | 7.0 | 7700 | 2100 |
| 3 | 1.12 | 0.86 | 89.5 | 116.0 | 10.0 | 7800 | 1900 |
| 4 | 0.86 | 0.66 | 116.0 | 151.9 | 11.0 | 7700 | 1700 |

**Table 3.** Summary of cold rolling experiments at Tata Steel pilot mill for the tinplate steel.

| Pass | $t_{in}$ (mm) | $t_{out}$ (mm) | $\sigma_{in}$ (MPa) | $\sigma_{out}$ (MPa) | $v_r$ (m/s) | Force (N/mm) | Torque (Nm) |
|---|---|---|---|---|---|---|---|
| 1 | 2.02 | 1.35 | 39.6 | 74.1 | 1.7 | 7000 | 2500 |
| 2 | 1.35 | 0.86 | 74.1 | 116.7 | 7.0 | 7500 | 2700 |
| 3 | 0.86 | 0.53 | 116.7 | 188.5 | 10.0 | 6800 | 2000 |
| 4 | 0.53 | 0.33 | 188.5 | 301.6 | 11.0 | 6000 | 1400 |
| 5 | 0.33 | 0.23 | 301.6 | 215.6 | 12.0 | 5600 | 1200 |

film[6] (equation (5)). It is important to note that $A$ is not a prescribed parameter but is computed as part of the coupled solution at each position in the roll bite, given the local roll pressure, lubricant film thickness, and surface roughness through the Wilson–Sheu asperity flattening constitutive relationship. The model inputs that require a priori characterization—the combined surface roughness $R_q$, the Johnson–Cook hardening constants, and the lubricant rheological parameters $\eta_0$, $\alpha$, $\beta$—are measured independently and are not fitted to the rolling force or torque data used for validation.

$$p = (1 - A)p_l + Ap_a$$

where $p_l$ is the hydrodynamic lubricant pressure and $p_a$ is the average pressure on contacting asperities.

The evolution of contact area fraction is determined using a triangular asperity height distribution assumed for both contacting bodies,[6] and the classical Wilson and Sheu model is adopted to describe asperity flattening.[18,19] This model provides a constitutive relationship between the contact area fraction and the corresponding contact pressure required to produce a given level of flattening. The Wilson–Sheu formulation has been widely validated against experimental observations[19,29] and offers a good balance between accuracy and computational efficiency.[26]

## Hydrodynamic behavior of the lubricant

Exploiting the thin-film approximation of the Navier–Stokes equations, the lubricant pressure distribution $p_l(x)$ in regions of hydrodynamic separation is determined by solving the Reynolds equation in its one-dimensional form appropriate for rolling (equation (6)):

$$\frac{dp_l}{dx} = \frac{12\eta}{\phi_x h_t^3}\left(\frac{v_r + v_s}{2}h_t + \frac{v_r - v_s}{2}R_q\phi_s - Q\right)$$

where $\eta$ is the dynamic viscosity, $h_t$ is the local film thickness, $v_r$ and $v_s$ denote roll and strip surface velocities, respectively, $Q$ is the volumetric flow rate per unit width, $R_q$ is the combined surface roughness (root mean square), and $\phi_x$ and $\phi_s$ are the pressure flow factor and shear flow factor, respectively, which account for the influence of surface roughness on the lubricant flow. The so-called average Reynolds equation approach, pioneered by Patir and Cheng,[22,23] allows the incorporation of surface roughness effects into the hydrodynamic analysis without requiring explicit resolution of the microscale geometry, through the mentioned flow factors. They account for the change in average flow compared to smooth surfaces due to the constriction of flow channels by asperities and are typically determined from numerical simulations of flow through rough surfaces.[22,23] For a given surface pattern (characterized by the ratio of correlation lengths in the rolling and transverse directions), the flow factors are functions of $h_t/R_q$, i.e., the film thickness normalized over the surface roughness. In the present implementation, analytical flow factors[47] for triangular surface roughness profiles aligned with the rolling direction are adopted.

The lubricant's viscosity is modeled as a function of its pressure and temperature through a Barus-type equation (equation (7)):

$$\eta = \eta_0 \exp(\alpha p_l - \beta T_l)$$

where $\eta_0$ is the viscosity at ambient conditions, $\alpha$ is the Piezo-viscous coefficient, and $\beta$ is the thermo-viscous coefficient.[30] The temperature $T_l$ in equation (7) is the lubricant temperature, determined from the thermal model. For higher pressure applications, the Roelands equation can be employed,[21] though an exponential relationship provides an adequate approximation for the moderate pressures encountered in the current validation cases. The implementation architecture is designed to allow straightforward substitution of alternative viscosity models, including those specific to water-based or polymer-solution lubricants, without modifying the core Reynolds equation solver. This flexibility enables rapid exploration of novel lubricant rheologies relevant to OFL development, where the viscosity behavior may differ substantially from conventional mineral oil emulsions.

Importantly, as noted by Boemer,[26] the average Reynolds equation holds as long as the lubricant pressure remains below the contact pressure between asperities. Beyond this threshold, it is assumed that the lubricant percolates through the contacting surfaces, which sets an upper limit to the achievable lubricant pressure. Consequently, upon reaching this condition, the fluid dynamics simplify to a flow rate conservation equation, and the lubricant pressure is set equal to the contact pressure at the interface.[26,33]

The shear stresses generated by lubricant viscosity and contact friction are likewise evaluated using a weighted average over the actual real contact area fraction $A$ (equation (8)):

$$\tau = (1 - A)\tau_l + A\tau_a$$

where $\tau_l$ is the viscous shear stress and $\tau_a$ is the frictional shear stress on contacting asperities.

## Elastic deformation of the rolls

Roll flattening significantly influences both the contact length and the distribution of contact pressure, particularly for rolling of thin strip where the contact length becomes

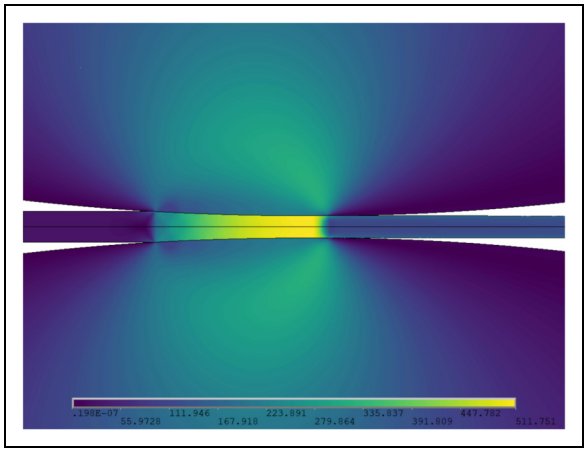

**Figure 2.** Von Mises equivalent stress distribution in the roll bite (deformation zone detail).

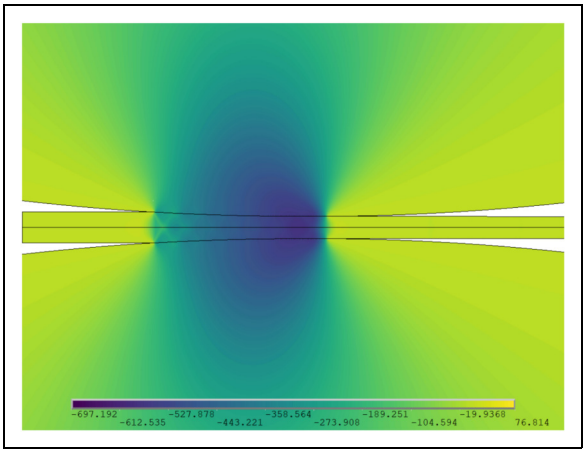

**Figure 3.** Normal stress distribution along the vertical direction in the roll bite detail.

an appreciable fraction of the roll circumference.[4,5] The elastic deformation of the work rolls is simulated using the classical Bland–Ford model,[4] which assumes that the local roll profile within the roll bite stays circular and that the local variation of the roll curvature radius within the roll bite is proportional to the normal force transmitted through the roll.

Non-circular models are known[2] to more accurately predict load distribution for sheet thicknesses under 0.4 mm, while cylindrical roll models are suitable for thicker sheets. Given that pilot mill tests are conducted at thicknesses above this threshold, the simplicity of the Bland–Ford model is appropriate. More sophisticated roll deformation models based on influence function methods[48] can be employed when higher accuracy is required for thin gauge rolling.

In CR1S, roll deformation is treated using the Bland–Ford extension[4] of Hitchcock's formula, which accounts for the effects of strip tensions and yield strength on the effective roll radius (equation (9)):

$$R' = R\left[1 + \frac{16(1-\nu^2)}{\pi E} 4.5cm \cdot \frac{P'}{\left(\sqrt{t_{\text{in}} - t_{\text{out}} + \delta_{\text{in}} + \delta_{\text{out}}} + \sqrt{\delta_{\text{out}}}\right)^2}\right]$$

where $R$ is the undeformed roll radius, $\nu$ and $E$ are Poisson's ratio and Young's modulus for the roll material, $P'$ is the rolling force per unit width, $t_{\text{in}}$ and $t_{\text{out}}$ are inlet and outlet strip thicknesses, and $\delta_{\text{in}}$ and $\delta_{\text{out}}$ represent the correction terms that adjust the flattened roll radius $R'$ to account for the contribution of the strip's elasticity to the roll deformation. This $R'$ defines the geometrical constraint for the roll bite, while the elastic deformation of the strip itself is resolved explicitly in CR1S through the spatial integration of the elastic constitutive equations in the inlet and outlet zones. This formulation provides a more accurate representation of the roll bite geometry compared to the classical Bland–Ford expression, particularly for thin strip rolling where entry and exit effects become significant.

This formulation also provides a computationally efficient approximation to the more complex problem of determining the roll profile by elastic analysis,[4] at the cost of assuming that the flattened profile remains circular with increased radius $R'$. While more sophisticated approaches based on influence function methods can capture local deviations from circularity, the Bland–Ford approximation has proven adequate for the moderate reductions typical of cold rolling, and its closed-form nature facilitates convergence of the iterative solution procedure.

## Thermal behavior of strip and lubricant

Thermal effects arise from two principal sources: plastic work dissipated in the strip, and frictional work at the interface.[8,21] It is considered that the plastic work done in the strip is (partially) converted into thermal energy of the strip alone, thereby increasing only the strip's temperature. Similarly, the viscous dissipation and shear stresses at the interface are assumed to be partially converted into thermal energy for the lubricant.[7,8] Knowing the densities and specific heats of both materials, it is thus possible to determine their temperature evolution throughout the roll bite. This thermal evolution, in turn, affects the physical properties of both strip and lubricant, resulting in a strongly coupled multiphysical model.[38] These assumptions are justified by the short residence time of strip and lubricant in the roll bite,[7] though heat conduction to the rolls becomes increasingly important at lower rolling speeds.

The rate of temperature rise of the strip due to plastic heating is thus (equation (10)):

$$\frac{dT_{\text{s}}}{dx} = \beta_{\text{s}} \frac{\dot{W}_{\text{p}}}{\rho_{\text{s}} c_{\text{s}} v_{\text{s}}}$$

where $\beta_{\text{s}}$ is the Taylor–Quinney coefficient (typically assumed in the literature to be 0.9, although it is known to be variable with the strain rate and accumulated plastic strain [49]; a value of 0.9 is adopted here), $\dot{W}_{\text{p}}$ is the plastic work rate per unit volume, $\rho_{\text{s}}$ and $c_{\text{s}}$ are the density and specific heat of the strip material, respectively.

The rate of temperature rise of the lubricant due to viscous friction at the interface is given by (equation (11)):

$$\frac{dT_{\text{l}}}{dx} = \beta_{\text{l}} \frac{1}{\rho_{\text{l}} c_{\text{l}} v_{\text{s}}} \frac{\tau_{\text{l}}(v_{\text{r}} - v_{\text{s}})}{h_{\text{t}}}$$

where $\beta_{\text{l}}$ is the fraction of friction energy dissipated into the lubricant thermal energy (approximately 0.1%, as determined

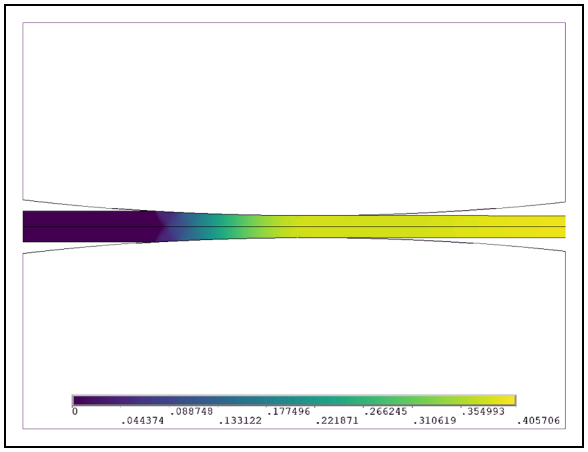


**Figure 4.** Accumulated plastic strain distribution in the roll bite detail.

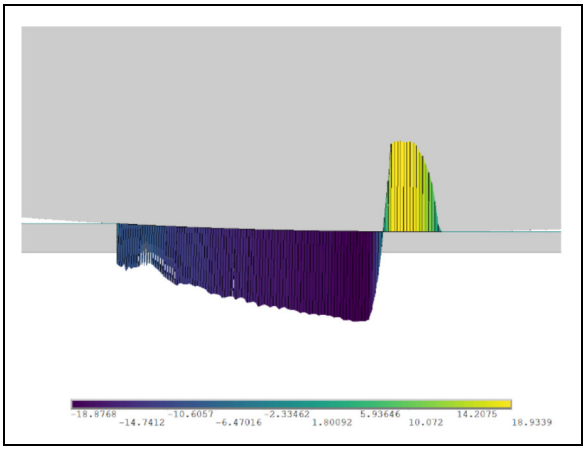


**Figure 5.** Contact shear stress distribution along the roll bite.

by Boemer et al.[26]; heat conduction to the rolls is neglected owing to the very short transit time of the strip through the roll bite[8,21]), $\rho_l$ and $c_l$ are the density and specific heat of the lubricant, respectively, $\tau_l$ is the interfacial shear stress (friction work rate), and $h_t$ is the local film thickness.

### *Iterative solution strategy*

The strong coupling between mechanical, tribological, and thermal phenomena necessitates an iterative solution strategy. The equations are integrated along the spatial coordinate in the direction of the strip's motion, starting from a point sufficiently far upstream of the roll bite and continuing through to its exit. To simulate a specific experimental scenario, an iterative solution procedure is implemented, similar to those described in previous one-dimensional rolling models.[26,33,34] The normal force, which in turn influences the deformed radius of the work roll and thus the deformed profile of the strip, is not known a priori; therefore, fixed-point iterations are carried out. The process begins by assuming an initial value of zero for the normal force, and at each iteration, the calculation is repeated using the updated force value from the previous iteration, until convergence is achieved.

Additional nested iterations ensure that: (i) the vertical position of the roll is determined such that the exit thickness of the strip matches the desired value using a bisection method; (ii) the strip velocity at entry is adjusted to satisfy the prescribed exit tension using a bisection method; and (iii) the lubricant flow rate entering the gap is determined as the value that satisfies the exit pressure condition (relative pressure of lubricant equals zero) using a bisection method.[26,33]

Typical solution times for a converged solution with 200 spatial points through the roll bite are in the order of a few seconds on a standard personal computer, making it particularly computationally efficient for both process design studies and real-time monitoring applications.[30]

## Validation against pilot mill trials and sensitivity analysis

### *Description of pilot trials*

The predictive capabilities of CR1S were assessed through comparison with experimental data obtained from pilot mill trials conducted at Tata Steel facilities (Figure 8). The trials encompassed a range of rolling speeds (1.7–12 m/s), reductions (21–38%), and strip thicknesses (0.232–2.520 mm), providing a comprehensive test of the model across industrially relevant conditions.

The pilot mill employed for validation consists of a two-high configuration with work roll diameter of 400 mm and a maximum rolling force of 2.0 MN. The strip material consisted of three different low-carbon steel grades: a soft steel (Table 1), a hard steel (Table 2), and a tinplate steel (Table 3), allowing investigation across a range of mechanical properties. Details of the experimental conditions are presented by Jacobs et al.[24]

Forward and backward tensions were applied to the respective strip faces. For all experiments, the reference oil lubricant was applied, ensuring full flooding conditions for all tests.

### *Validation results*

A very high level of accuracy is observed in the prediction of normal force and torque (as shown in Figures 9–11), which is not matched by an equally high accuracy in the prediction of forward slip. However, the overall trends in forward slip are correctly captured, and the associated errors remain limited. The predicted errors are comparable with those of state-of-the-art models described previously[26,30,36] and represent an important validation of the proposed one-dimensional model.

The reduced prediction accuracy observed for forward slip relative to rolling force and torque is a well-known limitation of one-dimensional slab models.[26,36] The neutral point position depends critically on the friction distribution in the roll bite and the lubricant inlet boundary conditions. The sensitivity analysis presented in Figure 12 corroborates this interpretation: modifications to lubricant viscosity and material yield stress produce large relative changes in forward slip compared to force and torque. Within the CR1S 1D framework, the elastic deformation of the strip in the inlet and outlet zones is resolved explicitly through the integration of the constitutive equations. The Bland–Ford $\delta_{in}$ and $\delta_{out}$ correction terms adjust the flattened roll radius $R'$ by accounting for the strip's elastic contribution to the roll deformation, defining the geometrical constraint for the 1D problem.

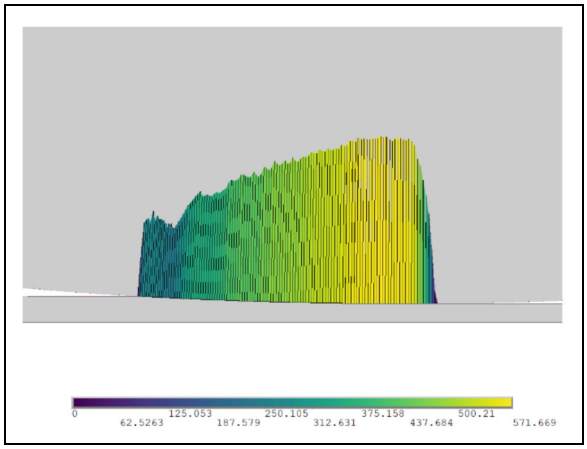


**Figure 6.** Contact pressure distribution along the roll bite; note the pressure peak at the inlet, which is not captured by 1D models.

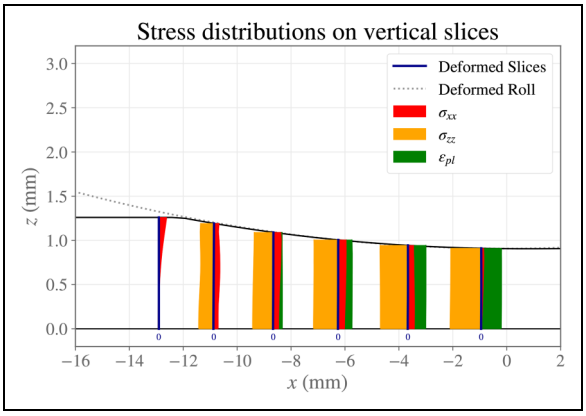


**Figure 7.** Distributions of longitudinal normal stress ($\sigma_{xx}$), vertical normal stress ($\sigma_{zz}$), and accumulated plastic strain ($\varepsilon_{pl}$) along vertical slices, with the deformed roll profile shown as a dashed line. Data magnitudes are normalized for relative comparison.




**Figure 8.** Photo of the pilot mill at Tata Steel.

The FE results (Figure 6) reveal a pressure peak at the inlet that is not fully captured by the 1D model despite the inclusion of strip elasticity, likely due to the inherent neglect of localized 2D stress concentrations in the slab method. This introduces uncertainty in the inlet film thickness boundary condition for the Reynolds equation, which is a primary contributor to the forward slip discrepancy. Furthermore, forward slip is fundamentally a differential quantity, calculated as the normalized difference between the predicted strip exit speed and the peripheral roll speed. This mathematical definition implies that even minor absolute errors in the predicted exit velocity are significantly amplified when expressed as a relative error in forward slip, inherently leading to higher percentage discrepancies compared to absolute integral parameters such as rolling force or torque.

The agreement between experimental and predicted rolling forces demonstrates the validity of the mechanical modeling approach, including the Johnson–Cook hardening law,[44] the slab method formulation,[4,14] and the Bland–Ford roll flattening model.[4] The torque predictions confirm that the friction modeling through the Wilson–Sheu asperity flattening approach[6,18] and Reynolds equation solution[7,22] captures the essential tribological behavior.

### *Sensitivity to lubricant properties*

Having the 1D simulator available where a constitutive model of the lubricant can be freely inserted as an input, it becomes straightforward to generate virtual experiments to explore the effect of changing physical properties on the process variables.[30,31] This becomes particularly important during the characterization phase of new lubricants, as it enables the possibility to chart development directions so that they are guided by quantitative performance metrics.[24]

The simulations related to the cold rolling of soft steel were repeated with three variations (Figure 12): in the first, the lubricant viscosity was set to a constant value ($\eta_0$ in equation (7)), independent of its pressure and temperature; in the second, the material's yield stress was increased by 20 MPa; in the third, the assumed surface roughness $R_q$ was increased by 20%. These changes do not have particularly significant effects on the torque required to drive the process, while they have a significant impact on the normal force and an even greater effect on the simulated forward slip. This points to the great influence of these parameters—affecting micro-plasto-hydrodynamic lubrication[30,31]—in the tribology of the cold rolling process.

## Discussion and conclusions

The one-dimensional model presented in this work demonstrates that a one-dimensional formulation, when carefully developed with appropriate treatment of mixed lubrication, thermal effects, and roll deformation, can provide accurate predictions of cold rolling behavior across industrially relevant parameter ranges. The validation against pilot mill data confirms that the maximum relative error in rolling force across all 13 experimental passes is less than 10%, based on the relative error $e_{\text{rel}} = |F_{\text{pred}} - F_{\text{exp}}|/F_{\text{exp}}$; the average relative error is approximately 5%. This demonstrates performance comparable to state-of-the-art one-dimensional models.[25,26,30,36]

A related methodological question concerns the consistency of the level of physical detail retained across the model's three coupled sub-models—mechanical, tribological, and thermal. The Bland–Ford roll-flattening model is an analytical circular-arc approximation known to be less accurate than non-circular, influence-function-based formulations, particularly for thin gauges.[2,48] One might ask whether the added complexity of the Johnson-–ook thermal-softening law and the full solution of the Reynolds equation is warranted, given that a simpler empirical friction correlation

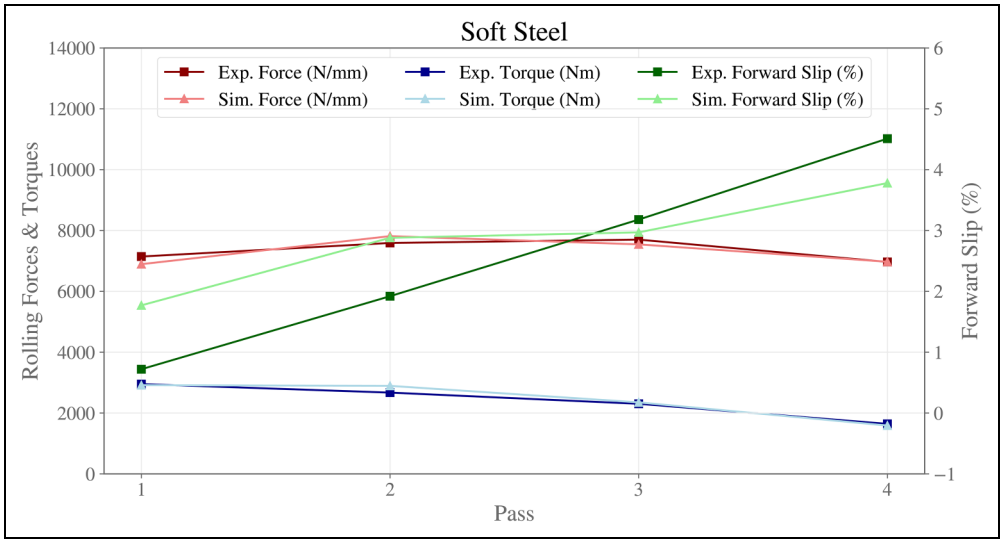


**Figure 9.** CR1S validation results for the soft steel: rolling force (N/mm), torque (Nm), and forward slip, comparing experimental data (markers) with model predictions (lines) across four passes.

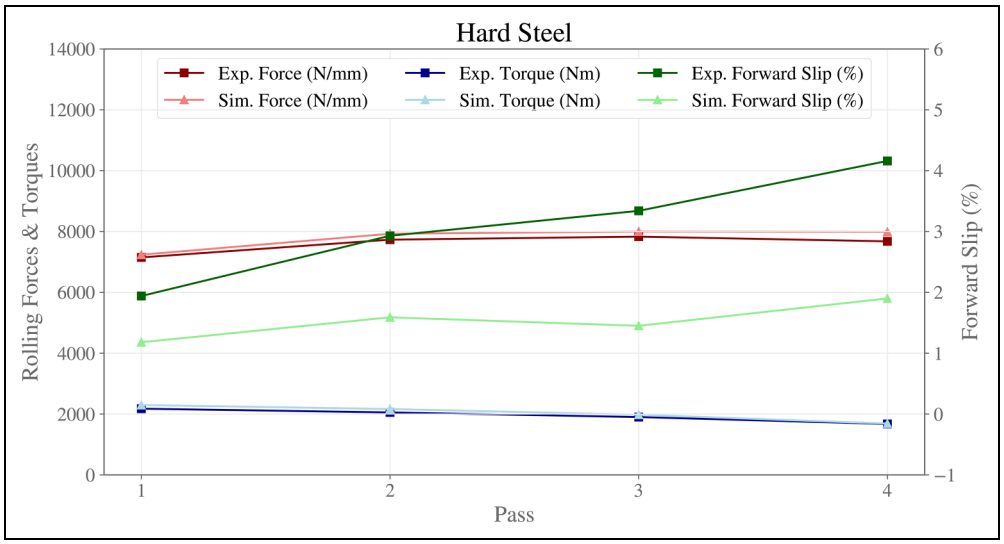


**Figure 10.** CR1S validation results for the hard steel: rolling force (N/mm), torque (Nm), and forward slip, comparing experimental data (markers) with model predictions (lines) across four passes.

and a lumped process-average temperature estimate could, in principle, be calibrated to reproduce rolling force to a comparable tolerance for a fixed mill, material, and lubricant. Rolling force and torque, however, are integral, spatially averaged quantities and are correspondingly forgiving of local modeling error, whereas forward slip and the interfacial friction distribution are first-order sensitive to the local balance between hydrodynamic and asperity contact pressure, and hence to the lubricant's viscosity–pressure–temperature behavior, as the sensitivity analysis of Figure 12 demonstrates. An empirical friction correlation calibrated against one lubricant and operating window would not transfer to a new lubricant formulation without re-calibration against new experimental data—precisely the capability CR1S is intended to provide for screening candidate OFL rheologies ahead of pilot trials.[24] The mechanical sub-model, being comparatively insensitive to the choice of lubricant, was accordingly retained at the simpler Bland–Ford level of fidelity. Notably, the average relative error in rolling force achieved here (approximately 5%) is at or below the level typically associated with Bland–Ford-based models, suggesting that the more detailed tribological and thermal treatment is consistent with, and may partly compensate for, the comparatively coarser mechanical sub-model, and not an unmatched addition of complexity. A systematic, quantitative ablation across the three sub-models—replacing each in turn with a lower-fidelity alternative and measuring the resulting loss of predictive accuracy—was not performed in the present work and is identified here as a valuable direction for future development.

The finite element analyses presented earlier provide confidence that through-thickness homogeneity is maintained in the work zone. However, the rapid changes in stress state occurring in the inlet and outlet zones are inherently more complex phenomena that may warrant future investigation through enhanced inlet/outlet models.[15,17]

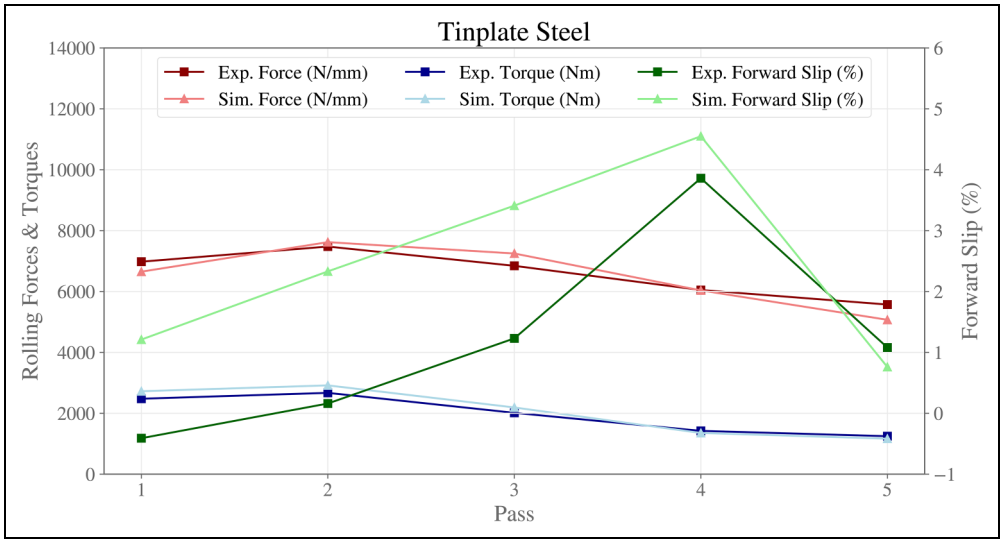


**Figure 11.** CR1S validation results for the tinplate steel: rolling force (N/mm), torque (Nm), and forward slip, comparing experimental data (markers) with model predictions (lines) across five passes.

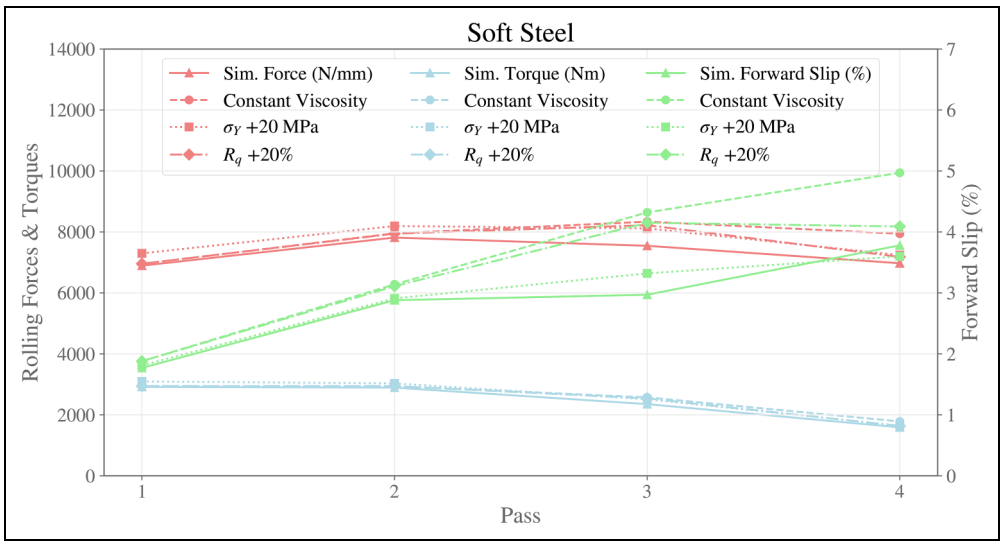


**Figure 12.** CR1S sensitivity analysis for the soft steel: effect of constant lubricant viscosity, +20 MPa yield stress offset, and +20% surface roughness ($R_q$) increase on predicted rolling force (N/mm), torque (Nm), and forward slip.

The asperity flattening model employed here, based on the Wilson–Sheu formulation,[6,18] has been validated primarily for steady-state conditions with relatively modest reductions. The analytical flow factors used in the average Reynolds equation (derived for triangular asperity profiles aligned with the rolling direction) are an appropriate idealization for freshly ground rolls, but may be less representative for more isotropic or worn surfaces or under boundary lubrication conditions where $h_t/R_q \to 0$. The forward slip prediction is also sensitive to the assumed surface roughness $R_q$: a variation of 10% to 20% in this parameter—within the typical scatter of profilometry measurements—produces comparable relative changes in predicted forward slip, while the effect on rolling force and torque remains modest (Figure 12). Recent work has highlighted the potential importance of transient asperity crushing phenomena[29,50] and the possibility that microscale lubricant pockets may persist through micro-plasto-hydrodynamic mechanisms.[30,31] Incorporation of these effects would require coupling the present macroscale model with microscale finite element analyses of representative surface elements,[26] an approach that has shown promise in recent research but remains computationally challenging for routine application.

While the Johnson–Cook model is well-suited for the cold rolling regime studied here, the CR1S architecture supports substitution of the constitutive law via a modular interface. This facilitates the integration of alternative formulations, including anisotropic yield functions such as Hill48, to account for the directionality of plastic behavior in cold-rolled steel grades; this extension, expected to improve accuracy for materials with significant plastic anisotropy, is planned as a direct next step and has been explored in related work.[31]

It is acknowledged that the present model operates under the steady-state assumption and does not account for the time-dependent evolution of roll surface roughness due to wear. Wear progressively alters $R_q$ and consequently affects

the contact area fraction $A$ and the entire lubrication solution. Coupling a wear model for the roll surface with the present steady-state framework represents an important direction for future research.

Despite these limitations, CR1S is a valuable tool to investigate the influence of lubricant formulations on cold rolling performance, which is precisely the objective it was developed for within the RollOilFree II project.[24] The computational efficiency enables extensive parametric studies and optimization of lubricant properties for specific rolling conditions. Note that, as formulated, CR1S is directly adaptable to multi-stand mills where the strip passes through multiple consecutive roll bites; it is sufficient to extend the integration of the related differential equations over a domain consisting of multiple roll bites, which requires a computational time increase that is linear with the number of passes.[30]

It should be emphasized that the validation reported here specifically targets offline virtual experimentation and lubricant screening for a specific pilot mill. While the computational speed of CR1S would in principle support online, closed-loop pass-scheduling or load-distribution presetting across arbitrary mills, materials, and lubricants, extending its validated range of applicability to substantially different mill geometries, steel chemistries, or operating windows would require either re-validation against additional experimental campaigns or, as discussed in the state of the art section, systematic comparison with data-driven approaches once suitable industrial process datasets become available. Because the model's constitutive inputs are measured independently, without fitting to the force and torque data used for validation (as detailed in the lubrication section), its predictions are expected to degrade gracefully under moderate extrapolation, governed by the physical plausibility of its governing equations; this expectation, however, has not been formally tested and is noted here as a limitation.

While the present validation covers three different steel grades under a conventional reference oil lubricant, the CR1S framework is not restricted to these conditions. The constitutive models for both the strip material and the lubricant are modular and replaceable; alternative hardening laws and rheological models—including those specific to water-based or polymer-solution OFLs—can be integrated without modifying the core numerical solver. Validation against additional materials and lubrication conditions forms the next step in the model's development within the ongoing RollOilFree II project.[24]

In conclusion, this work demonstrates that carefully formulated one-dimensional models remain valuable tools for cold rolling analysis, offering an effective balance between computational efficiency and physical fidelity that is well-suited to both research and industrial applications.[1,9] The validation presented provides confidence in the model's predictions across a range of conditions relevant to industrial practice, while the identified limitations and planned extensions chart a course for continued development toward even more comprehensive and accurate process simulation.

## Acknowledgments

This work was carried out within the project entitled "Transfer of aqueous oil free lubricants into steel cold rolling practice" (Ref. RollOilFree II, Grant Agreement No. 101112433) that has received funding from the Research Fund for Coal and Steel of the European Union, which is gratefully acknowledged. The sole responsibility of the issues treated in the present paper lies with the authors; the Commission is not responsible for any use that may be made of the information contained therein.

The authors also gratefully acknowledge Tata Steel for providing access to pilot mill facilities and for valuable discussions regarding experimental planning and data interpretation.

## ORCID iDs

Valentina Colla https://orcid.org/0000-0002-9574-0575
Tommaso Grossi https://orcid.org/0000-0002-2756-2893

## Funding

The authors disclosed receipt of the following financial support for the research, authorship, and/or publication of this article: This research was funded by the Research Fund for Coal and Steel (RFCS), Grant Agreement No. 101112433 (RollOilFree II).

## Declaration of conflicting interests

The authors declared no potential conflicts of interest with respect to the research, authorship, and/or publication of this article.

## References

1. Montmitonnet P, Fourment L, Ripert U, et al. State of the art in rolling process modelling. *BHM Berg Hüttenmänn Monatsh* 2016; 161: 396–404. DOI: 10.1007/s00501-016-0520-4.
2. Lenard J (ed) *Metal forming science and practice*. Elsevier Science, 2002.
3. Van Liempt P. Workhardening and substructural geometry of metals. *J Mater Process Technol* 1994; 45: 459–464. DOI: 10.1016/0924-0136(94)90382-4.
4. Bland DR and Ford H. The calculation of roll force and torque in cold strip rolling with tensions. *Proc Inst Mech Eng* 1948; 159: 144–163. DOI: 10.1243/PIME_PROC_1948_159_015_02.
5. Hitchcock JH. Elastic deformation of rolls during cold rolling. In: *Roll Neck Bearings*. New York: American Society of Mechanical Engineers, 1935, pp.33–41.
6. Sutcliffe MPF and Johnson KL. Lubrication in cold strip rolling in the 'mixed' regime. *Proc Inst Mech Eng B: J Eng Manuf* 1990; 204: 249–261. DOI: 10.1243/PIME_PROC_1990_204_064_02.
7. Wilson WRD and Murch LE. A refined model for the hydrodynamic lubrication of strip rolling. *J Lubr Technol* 1976; 98: 426–431. DOI: 10.1115/1.3452877.
8. Wilson W and Walowit J. An isothermal hydrodynamic lubrication theory for strip rolling with front and back tension. In *Tribology convention; institution mechanical engineers*. Institution of Mechanical Engineers, 1971, pp.164–172.
9. Button ST. Numerical and experimental analysis of lubrication in strip cold rolling. *J Braz Soc Mech Sci Eng* 2011; 33: 189–196. DOI: 10.1590/S1678-58782011000200010.
10. Cometa A. *Experimental and numerical study of pinching phenomena in sheet metal rolling processes*. PhD Thesis, University of Twente, Enschede, The Netherlands, 2023. doi: 10.3990/1.9789036556125
11. Li L, Xie H, Liu T, et al. Effects of rolling force on strip shape during tandem cold rolling using a novel multistand finite

element model. *Steel Res Int* 2022; 93: 2100359. DOI: 10.1002/srin.202100359.
12. Richelsen AB and Tvergaard V. 3D analysis of cold rolling using a constitutive model for interface friction. *Int J Mech Sci* 2004; 46: 653–671. DOI: 10.1016/j.ijmecsci.2004.05.013.
13. Boman R and Ponthot JP. Finite element simulation of lubricated contact in rolling using the arbitrary Lagrangian–Eulerian formulation. *Comput Methods Appl Mech Eng* 2004; 193: 4323–4353. DOI: 10.1016/j.cma.2004.01.034.
14. Karman T. Beitrag zur Theorie des Walzvorganges. *Z Angew Math Mechanik* 1925; 5: 139–141.
15. Flanagan F, O'Connor AN, Erfanian M, et al. Careful finite element simulations of cold rolling with accurate through-thickness resolution and prediction of residual stress. ArXiv:2408.03242 [cond-mat], 2024. DOI: 10.48550/arXiv.2408.03242
16. Flanagan F. *Mathematical modelling of the cold-rolling process*. PhD Thesis, University of Limerick, 2025. Artwork Size: 20158090 Bytes. DOI: 10.34961/RESEARCHREPOSITORY-UL.28631906.V1.
17. Sa CY and Wilson WRD. Full film lubrication of strip rolling. *J Tribol* 1994; 116: 569–576. DOI: 10.1115/1.2928884.
18. Wilson WRD. Friction models for metal forming in the boundary lubrication regime. *J Eng Mater Technol* 1991; 113: 60–68. DOI: 10.1115/1.2903383.
19. Sutcliffe MPF. Surface asperity deformation in metal forming processes. *Int J Mech Sci* 1988; 30: 847–868. DOI: 10.1016/0020-7403(88)90010-0.
20. Lin J, Huang T and Hsu C. Evaluation of lubricants for cold strip rolling. *Wear* 1991; 147: 79–91.
21. Liu YJ and Tieu AK. A thermal mixed film lubrication model in cold rolling. *J Mater Process Technol* 2002; 130–131: 202–207. DOI: 10.1016/S0924-0136(02)00720-3.
22. Patir N and Cheng HS. An average flow model for determining effects of three-dimensional roughness on partial hydrodynamic lubrication. *J Lubr Technol* 1978; 100: 12–17. DOI: 10.1115/1.3453103.
23. Patir N and Cheng HS. Application of average flow model to lubrication between rough sliding surfaces. *J Lubr Technol* 1979; 101: 220–229. DOI: 10.1115/1.3453329.
24. Jacobs L, Rèche D, Bán A, et al. Development of oil-free lubricants for cold rolling of low-carbon steel. *Processes* 2025; 13: 1234.
25. Liu S, Lu H, Zhao D, et al. Dynamic rolling force modeling of cold rolling strip based on mixed lubrication friction. *Int J Adv Manuf Technol* 2020; 108: 369–380. DOI: 10.1007/s00170-020-05259-0.
26. Boemer D, Carretta Y, Laugier M, et al. An advanced model of lubricated cold rolling with its comprehensive pilot mill validation. *J Mater Process Technol* 2021; 296: 117175. DOI: 10.1016/j.jmatprotec.2021.117175.
27. Hacquin A, Montmitonnet P and Guillerault JP. A steady state thermo-elastoviscoplastic finite element model of rolling with coupled thermo-elastic roll deformation. *J Mater Process Technol* 1996; 60: 109–116. DOI: 10.1016/0924-0136(96)02315-1.
28. Lin HS, Marsault N and Wilson WRD. A mixed lubrication model for cold strip rolling – Part I: Theoretical. *Tribol Trans* 1998; 41: 317–326. DOI: 10.1080/10402009808983754.
29. Sutcliffe MPF. Flattening of random rough surfaces in metal-forming processes. *J Tribol* 1999; 121: 433–440. DOI: 10.1115/1.2834086.
30. Jacobs L, Van Der Lugt J and De Rooij M. Contribution of viscous shear to friction in cold rolling of low-carbon steel. *Tribol Int* 2024; 191: 109102. DOI: 10.1016/j.triboint.2023.109102.
31. Jacobs L, Atzema E, Moerman J, et al. Quantification of the influence of anisotropic plastic yielding on cold rolling force. *J Mater Process Technol* 2023; 319: 118055. DOI: 10.1016/j.jmatprotec.2023.118055.
32. Jacobs L, Dam KV, Wentink D, et al. Effect of asymmetric material entrance on lubrication in cold rolling. *Tribol Int* 2022; 175: 107810. DOI: 10.1016/j.triboint.2022.107810.
33. Marsault N. *Modélisation du régime de lubrification mixte en laminage à froid*. PhD Thesis, École Nationale Supérieure des Mines de Paris, 1998.
34. Stephany A. *Contribution à l'étude numérique de la lubrification en régime mixte en laminage à froid*. PhD Thesis, Université de Liège, 2008.
35. Stephany A, Ponthot JP, Collette C, et al. Efficient algorithmic approach for mixed-lubrication in cold rolling. *J Mater Process Technol* 2004; 153-154: 307–313. DOI: 10.1016/j.jmatprotec.2004.04.310.
36. Carretta Y, Boman R, Stephany A, et al. MetaLub – a slab method software for the numerical simulation of mixed lubrication regime in cold strip rolling. *Proc Inst Mech Eng J: J Eng Tribol* 2011; 225: 894–904. DOI: 10.1177/1350650111410126.
37. Carretta Y. *Modélisation expérimentale et numérique du laminage à froid lubrifié en vue de la compréhension des phénomènes physiques et du développement d'un contrôle de lubrification flexible*. PhD Thesis, Université de Liège, 2014.
38. Montmitonnet P. Hot and cold strip rolling processes. *Comput Methods Appl Mech Eng* 2006; 195: 6604–6625. DOI: 10.1016/j.cma.2005.10.014.
39. Slimani K, Zaaf M and Balan T. Accurate surrogate models for the flat rolling process. *Int J Mater Form* 2023; 16: 23. DOI: 10.1007/s12289-023-01744-5.
40. Li J, Zhou J, Sun Y, et al. Interpretable machine learning-based rolling force prediction using multivariate industrial data during tandem cold rolling. *Ironmak Steelmak* 2025; 0: 0–0. DOI: 10.1177/03019233241310711.
41. Li J, Wang X, Yang Q, et al. Rolling force prediction in cold rolling process based on combined method of T-S fuzzy neural network and analytical model. *Int J Adv Manuf Technol* 2022; 121: 4087–4098. DOI: 10.1007/s00170-022-09567-5.
42. Gao Z, Wu S, Zhou X, et al. Physics-informed machine learning of rolling forces and its application to the optimization of rolling schedules. *J Manuf Process* 2025; 153: 138–150. DOI: 10.1016/j.jmapro.2025.09.007.
43. Wang Z, Zhang J, Wang Z, et al. Physics-informed and MC dropout-based sequence prediction for cold tandem rolling: towards rolling schedule presetting and uncertainty quantification. *Measurement* 2026; 269: 120833. DOI: 10.1016/j.measurement.2026.120833.
44. Johnson GR and Cook WH. A constitutive model and data for metals subjected to large strains, high-strain rates and high-temperatures. In: *Proceedings of the 7th International Symposium on Ballistics*, The Hague, Netherlands, 19–21 April 1983, pp. 541–547. Arlington, VA: American Defense Preparedness Association.
45. Roberts WL. *Cold rolling of steel*. Marcel Dekker, 1978.
46. Greenwood JA and Williamson JBP. Contact of nominally flat surfaces. *Proc R Soc Lond A, Math Phys Sci* 1966; 295: 300–319. DOI: 10.1098/rspa.1966.0242.
47. Wilson WRD and Chang Df. Low speed mixed lubrication of bulk metal forming processes. *J Tribol* 1996; 118: 83–89. DOI: 10.1115/1.2837096.

48. Jortner S, Osterle JF and Zorowski CF. An analysis of cold strip rolling. *Int J Mech Sci* 1960; 2: 179–194. DOI: 10.1016/0020-7403(60)90003-5.
49. Dæhli LEB, Johnsen J, Berstad T, et al. An experimental–numerical study on the evolution of the Taylor–Quinney coefficient with plastic deformation in metals. *Mech Mater* 2023; 179: 104605. DOI: 10.1016/j.mechmat.2023.104605.
50. Tomilo VA, Pilipenko SV, Dudan AV, et al. Method for determination of the friction coefficient during cold rolling of extra thin sheets. *J Frict Wear* 2024; 45: 147–151. DOI: 10.3103/S1068366624700223.